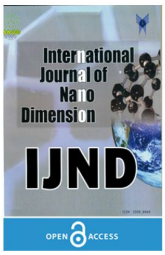

Volume 15, Issue 2, 152409 (1-12)

International Journal of Nano Dimension (IJND)

https://doi.org/10.57647/j.ijnd.2024.1502.09

The astonishing ultra-small iron oxide nanoparticles as positive contrast agents for MR Imaging of cancerous tissues: A review

Azadeh Amraee[1], Abolfazl Sarikhani[2], Samira Rasaneh[1]*

[1]*Social Determinants of Health Research Center, School of Medicine, Lorestan University of Medical Sciences, Khorramabad, Iran.*
[2]*Finetech in Medicine Research Center, Iran University of Medical Sciences, Tehran, Iran.*

***Corresponding author:** srasaneh@gmail.com

REVIEW PAPER

Received:
12 December 2023
Revised:
16 February 2024
Accepted:
17 February 2024
Published online:
30 March 2024

Abstract:

Magnetic nanoparticles, which make up a large part of nanomaterials, have the potential for clinical diagnosis and treatment due to their unique properties such as magnetic and superparamagnetic torque and the power of biological interactions at the cellular and molecular levels. The unique properties of these nanoparticles include super-saturation, superparamagnetic and magnetic susceptibility, which are derived from their inherent magnetic properties. In this review, we investigated the properties of ultra-small iron oxide nanoparticles as a positive contrast agent in MRI. As a result, ultra-small iron oxide nanoparticles have a high potential for use as a T_1 weight contrast agent in the clinic. Ultra-small iron oxide nanoparticles have been widely used as a contrast agent in MR imaging. In ultra-small iron oxide nanoparticles, it has been shown that the states change from superparamagnetic to paramagnetic by decreasing in size. Therefore, it can be said that as a result of reducing the size of these nanoparticles, they change from being the T_2 contrast agent to a T_1 contrast agent. Unlike iron oxide nanoparticles larger than 5 nm, these nanoparticles can create a positive contrast that will facilitate detection. Also, ultra-small iron oxide nanoparticles could solve the problem of gadolinium toxicity and the high magnetic momentum of iron oxide. As a result, this nanoparticle has a high potential for use as a T_1 weight contrast agent in the clinic.

Keywords: Contrast agent; Magnetic nanoparticles; MRI; Relaxation times; T_1-weighted; Ultra-small iron oxide

1. Introduction

The highest rate of mortality in the world is still caused by cancer despite progress in treating and diagnosing the disease [1, 2]. Proper diagnosis is important to facilitate treatment. To obtain effective treatment, we need a diagnostic system that can detect the lesion in the early stages. Imaging techniques such as MRI and CT-Scan can show lesions accurately with an accuracy of -2.4 mm [3]. However, these methods are not able to detect malignancies in the early stages and at the cellular level. The use of molecular imaging methods is needed because of this. The use of nanoparticles in medicine has become widespread, especially in diagnostic devices. The development of nano complexes is a very serious idea in nanotechnology so that these nano complexes can remain in the circulatory system for a long time and at the same time have therapeutic potential. To use nanotechnology in practical medicine, magnetic nanoparticles have been proposed as a class of non-invasive nanomaterials for various biomedical applications. In particular, magnetic nanoparticles have been considered by researchers for the effective diagnosis of diseases. Various modifications have been made to magnetic nanoparticles so that they can be used to communicate with the biomass of molecules and interact with the target tissue. As a result, the market is witnessing the development of a new generation of nanomaterials that have low toxicity and high diagnostic capabilities which can help in the early diagnosis of diseases [4].

2. Magnetic resonance imaging (MRI)

MRI has a unique feature in imaging because it has such features as no restriction on tissue penetration, high spatial resolution (1 mm), high soft tissue contrast and also safety due to the non-use of ionizing radiation is a medical diagnosis [5, 6]. It is used in a wide range of applications, including imaging-guided drug delivery [7, 8], Alzheimer's [9], angiography [10], pH measurement [11], liver disease [12], and tumor diagnosis [13–15]. However, the main drawback of this imaging method is its low sensitivity [16]. It is estimated that 40 to 50% of MRI imaging, and especially tumor imaging, uses contrast media to increase sensitivity [15, 17, 18].

2.1 MRI contrast agents

The contrast mechanism in MRI is much stronger than other imaging methods due to differences in proton density, longitudinal (T_1), and transverse (T_2) relaxation times. MRI is the most powerful imaging technique. Due to the small difference between the longitudinal and transverse relaxation times of normal and abnormal tissues, the use of contrast agents can help to identify these tissues, better display the circulatory system and show the blood-brain barrier. Therefore, there is still a need to use contrast agents in MRI. The resulting image depends on the magnetization vector, which is the result of the ratio of spins in two directions parallel to the field and non-parallel to the field. The parameters that determine the ratio of the number of spins up to the spin down are obtained from the following equation:

$$\frac{(\neq spinup)}{(\neq spindown)} = \exp\left[\frac{\gamma h B_0}{KT}\right] \qquad (1)$$

In this formula:
γ : Gyromagnetic ratio (Hz / Tesla)
h : Planck constant (6.626×10^{-34} J sec)
B_0 : External magnetic field (Tesla)
k : Boltzmann constant (1.381×10^{-34} J / K)
T : Temperature in Kelvin (K)

Since changes such as viscosity and temperature are required to increase this ratio, these parameters can't be changed in clinical studies and can only be changed in laboratory conditions. Besides the parameters mentioned above, chemical properties such as proton density and comfort periods also play a role in image formation. In the clinic, these parameters can be changed - especially changes in relaxation times with the use of contrast agents - to improve the display of tissue. Contrast agents change signal intensities and cause differences in signal intensities in different tissues [19]. The nature of the contrast agents is different in CT and MRI. In CT, contrast agents act directly through their ability to absorb and scatter photons. X-ray attenuation on CT is simply the sum of the attenuation of the tissue and the contrast agent. MR contrasts act indirectly by changing the local magnetic environment of the tissue, leading to changes in relaxation patterns. A contrast agent that increases the signal received from the patient is a positive contrast agent and any substance that decreases the signal received from the image is a negative contrast agent [20].

2.1.1 Classification of contrast materials in MRI

The properties of contrast agents in MRI can be classified into several categories:

1) Magnetic properties of matter (paramagnetic and superparamagnetic).

2) The effect of the contrast agent on the signal strength of the signal increases (positive contrast) and decreases the signal (negative contrast) [21–25].

Contrast agents in MRI affect both T_1 and T_2 parameters, but their effect is usually greater on one of the T_1 and T_2 parameters. Thus, the contrast agents are divided into two groups of reducing agents, T_1 and T_2. Decreasing the longitudinal relaxation time of the proton causes a rapid increase in the longitudinal magnetization vector, followed by an increase in the signal in the images. Hence, T_1 time-reducing materials are called positive contrast agents, which can be brighter seen in T_1-weighted images [20].

2.1.2 Mechanism of the effect of contrast agents on relaxation times T_1 and T_2

In MRI, the difference in the intensity of the magnetic resonance signal of the tissue in the image is called contrast. This discrepancy should be sufficient to be able to identify and determine anatomical and pathological evidence. The contrast observed in MR images (without contrast agent) changes with N (H) spin density, relaxation times T_1 and T_2, resonant frequency, chemical shift, magnetic susceptibility, and other molecular stimuli. The variables affecting the signal strength are proton spin density, spin-lattice relaxation time or longitudinal relaxation time T_1, and spin-spin relaxation time or transverse spin relaxation time T_2. In addition to the proton, which has a direction in the magnetic field due to the presence of spin, and in principle, from the same behaviors in the magnetic field, a signal is obtained, another particle called an electron also has a direction in the magnetic field, and since it has a negative charge, its direction will be opposite to that of a proton. The more electrons in an atom, the stronger the electron cloud forms around the nucleus, and the fewer protons are affected by the external field. Less impact on the field means fewer longitudinal and transverse relaxation times. This is why we see hydrogen relaxation times in fat are shorter than hydrogen relaxation times in water. In addition, due to the lower electron cloud in the hydrogen of the water molecule, the protons, in addition to spin-spin rotate, rotate around the axis of their molecule, which is called wobble. Paramagnetic and superparamagnetic materials have unpaired electrons in their orbital alignment. These orbital electrons can absorb hydrogen in the water molecule. Hydrogen is trapped in a macromolecule by this method. The wobbling rate of water molecules decreases, and the amount of hydrogen proton magnetization decreases. As a result, the relaxation time for this proton is shortened. In this way, the phenomenon of increased contrast is visible in the image. Gadolinium, for example, has seven unpaired electrons (more than any other element) and produces a large magnetic moment (approximately seven hundred times that of a proton) and in connection with dipole-dipole interaction causes faster relief and shorter T_1 and due to the direct relationship leads

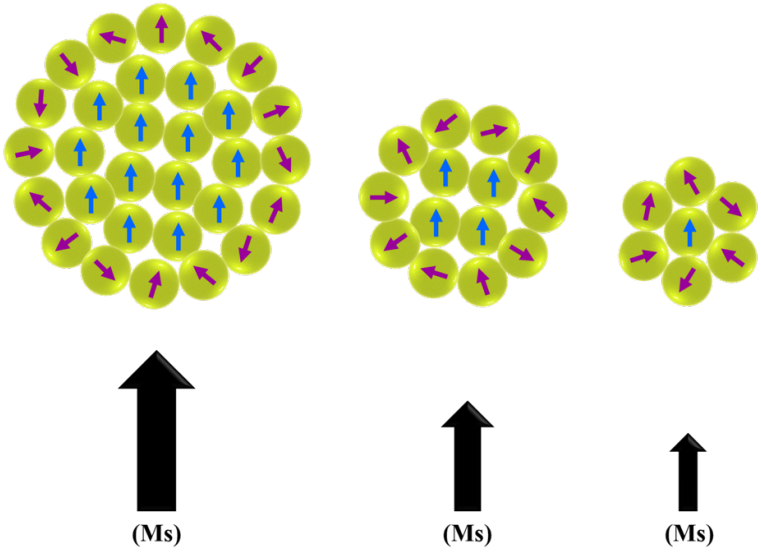

Figure 1. As the size of iron oxide magnetic nanoparticles decreases, the magnetic momentum also decreases.

to an increase in signal strength. The paramagnetic effect is expressed by relaxation or r. It is generally calculated in water and 1 mmol of the substance. Relaxation or r is the slope of the linear relationship between the rate of proton relaxation and the concentration of the contrast agent. Positive contrast leads to the brightening of the image of the target tissue after administration of the drug, while negative contrast leads to darkening. Nanoparticles reduce the time of the T_1 and T_2 cycles with their small structure. Paramagnetic nanoparticles in the magnetic field used in MRI are magnetically saturated and can produce a local disruptive dipole field, thus reducing the values of T_1 and T_2.

In the absence of contrast agents, there are inherent proton relaxation patterns in the tissue. Following the administration of a contrast agent, the observed relaxation times are the linear sum of the intrinsic relaxation time of the tissue and the contrast agent:

$$\frac{1}{T_{1,2\,(\text{observed})}} = \frac{1}{T_{1,2\,(\text{intrinsic})}} + \frac{1}{T_{1,2\,(\text{contrastagent})}} \qquad (2)$$

The concentration of the paramagnetic sample is crucial here. The following equation describes the relationship between the concentration of samples and $\frac{1}{T_{1,2\,(\text{intrinsic})}}$:

$$\frac{1}{T_{1,2\,(\text{observed})}} = \frac{1}{T_{1,2\,(\text{intrinsic})}} + r_{1,2}[C] \qquad (3)$$

In the last equation, C is concentration, and $r_{1,2}$ is related to the T_1 and T_2 relaxation of the paramagnetic sample. The r parameter is a measure of the ability of a contrast agent sample to act on relaxation times and is expressed in $mM^{-1}s^{-1}$. Here the concentration is expressed in millimoles per liter (millimeters or mM) and the relaxation time is expressed in s^{-1} (per second). Currently, most of the contrast agents used in the clinic is based on the paramagnetic chelates of lanthanide metals such as gadolinium. The presence of paramagnetic ions near water protons reduces their T_1 comfort time through coordination with water molecules and increases contrast. Although gadolinium chelates are widely used, their short circulation time, poor tracking sensitivity, and toxicity concerns, especially in the kidneys, have led to the widespread development of magnetic nanoparticles as contrast enhancers [27].

3. Magnetic nanoparticles

The increase in T_1 for ultra-small iron oxide nanoparticles has been attributed to a number of factors, including surface increase, decrease in magnetization, and surface coverage. The surface effects are the most obvious change after reducing the nanoparticle's size. The spins of a magnetic nanoparticle can be thought of as a shell-core structure, which, as it decreases in size, the surface spins of the nanoparticle become skewed or irregular, which is due to incomplete coordination or symmetry. This causes us to have a dead magnetic layer on the surface of the ultra-small nanoparticles. This effect reduces the magnetization of the nanoparticles. The responsibility for magnetization falls on the necks of regular spins at the center, which drastically reduces the function of the magnetic nanoparticle as a T_2 contrast agent (Figure 1). The magnetic properties of nanoparticles shift from superparamagnetic to paramagnetic. Reducing the magnetization dramatically reduces r_2 and, by nature, the r_2 / r_1 ratio, which makes this ultra-small iron oxide nanoparticle suitable as a positive contrast agent (Figure 2) [26].

3.1 Considerations in the design of magnetic nanoparticles to enter the body

Although there has been significant progress in the quality of magnetic nanoparticles, design factors must be considered at each stage of the manufacturing process to increase the chances of reaching the target cells (by increasing the lifespan of the nanoparticles and increasing their entry into the cells). Potentially, the intrinsic properties of magnetic nanoparticles are used in hyperthermia and MRI. Nanoparticles are used in the field of treatment and imaging methods

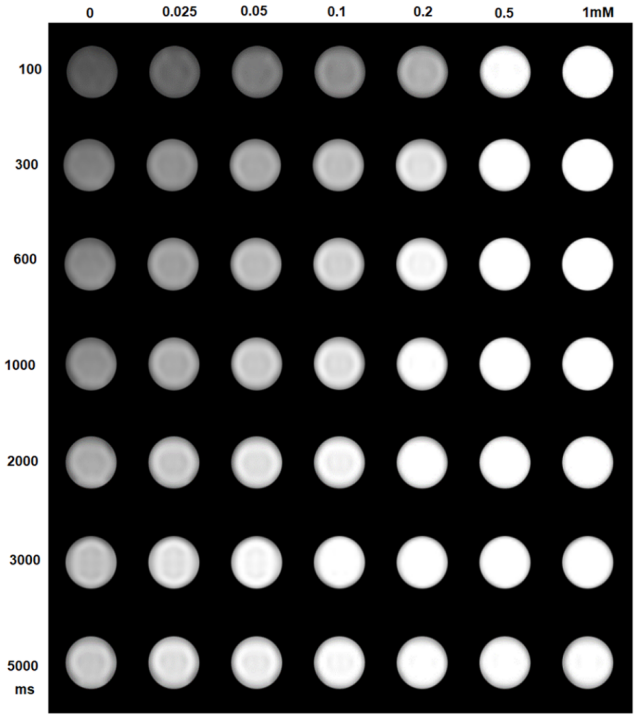

Figure 2. Ultra-small iron oxide nanoparticles as positive contrast agents for MRI images in different TRs (from 100 to 5000) and concentrations of 0.025, 0.05, 0.1, 0.2, 0.5, and 1 mM and water as a control group [26].

due to their high surface-to-volume ratio and are also well-studied [28]. In practice, achieving appropriate therapeutic and diagnostic results is strongly influenced by the set of biological barriers that nanoparticles face in a very complex body system. Biochemical barriers prevent them from reaching their target, so in most cases, 5% or less of the injected nanoparticles reach the tumor tissue and most of the injected dose accumulates in healthy tissues, causing side effects in the limb. In addition, nanoparticles encounter cellular barriers (such as cell membranes and endosomes/lysosomes) to cross the cell gate to reach the target cell [29]. Optimization of the physical and chemical properties of nanoparticles in nanostructures has an important role in the design of conventional nanoparticles according to extensive research.

3.1.1 Overcoming the endocytosis barrier

3.1.1.1 Passive targeting

In addition to all of the design considerations that increase the lifespan of nanoparticles in the blood to reach tumor cells, these carriers must undergo a process called ”endocytosis” to deliver the drug to cancer cells. In particular, the accumulation of nanoparticles in the tumor using physical and chemical properties as well as enhancement and maintenance of permeability (EPR) was the first investigated by Meda *et al.*, in 1986 in metastatic solid tumors [30]. Nanosystems can use the structural features of tumor tissue for passive targeting. When the tumor size to 2 mm or more, it becomes permeable. This limit impacts the capacity of cells to soak up food, waste, and oxygen. Tumor tissue initiates the vascular process to overcome this problem. Characteristics of this phenomenon include abnormalities in the basement membrane and discontinuous epithelium that result in the formation of leaking vessels containing pores between 20 and 2000 nanometers in size. The length of the pores varies relying at the kind of tumor. In addition, due to the lack of basal kidneys from the cavities of the efficient lymphatic system in the tumor tissue, the interstitial pressure in the center of the tumors is greater than in the surrounding environment. This increase in internal pressure causes an outflow of interstitial fluid, thereby reducing the spread of the drug to the center of the tumor. It has been shown that tumor tissue can trap plasma proteins and use the products of their decomposition to grow. The most common example of passive targeting in the treatment of tumors is increasing and maintaining the effect of permeability. This feature is based on two features of tumor tissue: 1) The arrangement of capillary endothelial cells in malignant tissue is more irregular than in healthy tissue and has a higher permeability than macromolecules. 2) Lack of lymphatic drainage in the tumor bed leads to drug entrapment in this area.

3.1.1.2 Active targeting

Despite all of the inactive targeting benefits and the use of EPR, complex biological processes such as vascular permeability, angiogenesis, and heterogeneity in the microscopic environment of the tumor somehow prevent the practical application of this effect. In addition, the biological, physical, and chemical properties of nanoparticles are affected by the quality of their distribution and accumulation in the tumor [31]. These reasons, along with the emergence of specific therapies; led to a reduction of the inactive targeting used and the flourishing of active targeting. Although the

active targeting method was proposed about 40 years ago [32], nanoparticles attached to ligands have recently made their way into potential experiments [33]. The increase in dependence and association with specific cells is achieved by the binding of nanoparticles equipped with targets whose complementary receptors are present on target cells. In this method, access to specific antigens on target cells is critical for proper binding to nanoparticles adorned with ligands. Ligands include antibodies, aptamers, proteins, peptides, and small molecules that bind specifically to the surface molecules or receptors in the target organs [34].

4. Review of the past works

In this section, an overview of past studies in 4 fields of using ultra-small iron oxide nanoparticles, large or superparamagnetic iron oxide nanoparticles, gadolinium, and the combination of iron and gadolinium in MRI imaging is given.

4.1 Ultra-small Fe_3O_4 nanoparticles in MRI as T_1-weighted contrast media

In a study conducted in 2004 by Schnoor *et al.*, in Germany on 3 pigs to investigate the effect of VSOP-C184 nanoparticles with a core size of 4 nm and a diameter of 7 nm on MRA images of 1.5 Tesla and with Gd- DTPA was compared, the r_1 and r_2 were 13.9 and 33.4 ($mM^{-1}s^{-1}$), respectively. The results showed that these nanoparticles had the ability to be used in MRA and also the ability to observe the artery without the intervention of venous signal [35].

In another study conducted by Kim *et al.*, in Korea in 2011, ultra-small iron oxide nanoparticles with a size of less than 4 nm were prepared by thermal decomposition method and their effects on MCF-7 cells and rat were investigated. The results obtained from 3 Tesla MRI images showed that r_1 and r_2/r_1 ratio were 4.78 and 6.12 ($mM^{-1}s^{-1}$), respectively, as well as high biocompatibility, less toxicity, and longer shelf life. Nanoparticles in blood circulation are superior to gadolinium-based contrast agents and showed the potential of ultra-small iron oxide nanoparticles to be used as a T_1-weighted contrast agent [36].

In 2017, Park *et al.*, in Korea prepared ultra-small iron oxide magnetic nanoparticles with a 3 nm iron oxide core and a PEG shell with a hydrodynamic size of 8 to 14 nm by thermal decomposition method and used them for angiography of the hearts of 9 dogs in two different sessions and 7 days apart, they were imaged by 3 Tesla MRA, the amount of r_1 and the r_2/r_1 ratio were 5.6 and 1.3 $mM^{-1}s^{-1}$, respectively, due to the many advantages of this nanoparticle compared to gadolinium-based materials, including their larger size compared to them, which are not quickly eliminated from the body and provide the possibility of obtaining angiographic images, they have less toxicity(due to the Gd^{3+} ion). They are also useful for the body and treat iron deficiency in the body, they have a high potential for use in MRA [37].

Another study in 2016 in China by Roy *et al.*, on ultra-small magnetic iron oxide nanoparticles and polyacrylic acid with a hydrodynamic size of 4.5 nm on rabbits and pigs, which MRA images of 1.5 tesla after the injection of 135 μmol/kg iron, r_1 and r_2/r_1 were 8.67 and 2.93 $mM^{-1}s^{-1}$, respectively, and the obtained results showed that PAA@USPIO nanoparticles have the ability to be used as contrast material with T_1 weighted in the clinic [38].

Another study was conducted by Shen *et al.*, in China on U-87 MG, MCF-7 cells, and Nod mice. DOX@ESMION3@RGD2@mPEG3 nanoparticles were prepared by co-precipitation method, the obtained results showed that these nanoparticles have the ability to be used as T_1 contrast enhancement agent and also, they can be used for targeted drug delivery to Tumor used [39]. In 2017, Vangijezgam *et al.*, in Belgium prepared two nanoparticles PEG2000-VSION and PEG750-VSION with a size of 3.5 nm by thermal decomposition method and took MRI images of 9.4 Tesla from CD1 mice with a concentration of 45 μmol Fe/kg. The results showed that this nanoparticle system has a high potential to be used as a weighted contrast agent due to their longer persistence in the blood circulation ($>$ 1 hour), and their clearance from the body, through the kidney and liver at the same time with T_1 weighted in MRA [40]. Another study was conducted in Germany in 2011 by Wagner *et al.*, in order to investigate the effect of ultra-small superparamagnetic iron oxide nanoparticles covered by citrate (VSOP-C184) in increasing the contrast of angiographic images of patients with suspected coronary problems; MRA images were obtained from 6 healthy volunteers and 14 patients after injection of contrast material and compared with images before injection, the results showed SNR from 15.4 to 21.7, CNR from 6.9 to 15.1, and VED from 1.2 increase to 2.3, and this shows that VSOP-C184 nanoparticles have the ability to accurately detect coronary occlusions [41].

Another study was conducted in America in 2017 on ultra-small iron oxide nanoparticles coated with zwitterion with a core size of 3 nm and a coating of 1 nm and a hydrodynamic size of 4.7 nm, which was prepared by thermal decomposition method. The MRI of 1.5 and 7 Tesla images were prepared and the r_1 and r_2/r_1 values obtained in the 1.5 tesla field were 2.5 $mM^{-1}s^{-1}$ and 2 $mM^{-1}s^{-1}$, respectively, and in the 7-Tesla field, 5.1 $mM^{-1}s^{-1}$ and 11 $mM^{-1}s^{-1}$ respectively. The obtained results showed that these nanoparticles have the proper size for excretion from the kidney system and also because of their greater biocompatibility, they have a high potential to be used as a T_1-weighted contrast agent in the clinic [42].

Another study was conducted by Li *et al.*, in 2019 on ultra-small pH-sensitive iron oxide nanoparticles. In this way, the ultra-small iron oxide nanoparticles were connected by aldehyde ligands, which were released in the acidic environment of the tumor, and the ultra-small iron oxide nanoparticles that were stuck together and had superparamagnetic magnetic properties and were negative contrast material, with taking a distance from each other, they change to paramagnetic state and the contrast material becomes positive. The amount of r_1 and the ratio of r_2/r_1 in the neutral pH state (pH=7.3) were equal to 2.3 $mM^{-1}s^{-1}$ and 33.8 $mM^{-1}s^{-1}$, respectively, and these values in the acidic state (pH=5.5) were respectively reached to1.5 $mM^{-1}s^{-1}$ and 4.2, which is an excellent idea in imaging, which makes

the contrast material increase the signal only in the acidic region of the tumor [43].

4.2 Fe_3O_4 nanoparticles as contrast agent in T_1 weighted MRI

In 2011, a study in Australia by Campbell and his colleagues to investigate the effects of iron oxide core-shell magnetic nanoparticles covered with silica, with a size of less than 100 nm invitro on PC3 cells and invivo on Nude mice done. The results showed that these nanoparticles can use as T_2-weighted contrast materials [44].

It's interesting to know that there was a study conducted in 2017 by Reguera and his colleagues in Spain to investigate the effects of star nanoparticles of iron oxide and gold. Apparently, these nanoparticles have the potential to be used in different imaging modalities such as CT Scan, photoacoustic imaging, and MRI. According to the study, the size of iron oxide in this nanocomplex ranged from 16 to 20 nm, and the hydrodynamic size was between 25 to 40 nm. The results obtained during the study showed that the obtained r_2 ranged between 180 and 300 $mM^{-1}s^{-1}$. Furthermore, the ratio of r_2 to r_1 obtained for 16 nm iron oxide nanoparticles was 20 to 30, and for 20 nm iron oxide, it was 40 to 50. These high potentials indicate that these nanoparticles are suitable to be used as T_2-weighted contrast agents in MRI [45].

It's interesting to know that in 2014, Sarasousi and his colleagues conducted a study in India on iron oxide nanoparticles coated with citrate, with a size of about 12 nm. The results showed that these nanoparticles had high stability and the r_2/r_1 ratio was 37.92. T_2-weighted MRI images showed the dependence of iron dose in rodent pulmonary fibrosis cells, and it was proved that these nanoparticles can be used as a T_2-weighted contrast material [46].

It's interesting to learn about Beck and his colleagues' recent study on a theranostic nanocomplex. Apparently, this nanocomplex comprises graphene oxide, gold nanoparticles, and superparamagnetic iron oxide. What's even more impressive is that this nanocomplex not only enhances contrast in MRI but also shows promising therapeutic potential in radiotherapy and photothermal therapy. The r_2 obtained from this study was equal to 62.92 $mM^{-1}s^{-1}$, which indicates that this biocompatible nanocomplex could be used for both diagnosis and treatment of cancer simultaneously [47].

4.3 Gd nanoparticles in MRI

In a 2017 study conducted by Mekuria and his colleagues in Taiwan, G4.5-Gd_2O_3-PEG nanoparticles were synthesized and their effects on RAW264.7 cells and BALB/c mice in a 7 Tesla field were investigated. The study found that the nanoparticles had an r_1 value of 53.9 $mM^{-1}s^{-1}$ and an r_2 value of 182.8 $mM^{-1}s^{-1}$, indicating their potential as a T_1-weighted contrast agent. The results also showed that the nanoparticles had a low toxicity and were biocompatible with the cells and mice tested. These findings recommend that Gd_2O_3-PEG nanoparticles could be a promising contrast agent for clinical applications in MRI [48].

It seems that the study conducted by Qaqada and his colleagues in America back in 2009 showed promising results for the use of liposomes based on gadolinium nanoparticles as a contrast agent, both in vivo and in vitro. The high ability of these nanoparticles to be used in this way is certainly a promising development [48].

It's interesting to see the potential of liposomes based on gadolinium nanoparticles as a contrast agent, as demonstrated by a study conducted by Ghaghada and his colleagues in America back in 2009. The testing that in vivo and in vitro showed promising results, indicating that these nanoparticles could be highly effective in this application. Specifically, the study showed that the nanoparticles exhibited a strong T_1 response [49].

Another interesting study on gadolinium nanoparticles as a contrast agent was conducted by Dai *et al.* in China in 2017. The study focused on PEG-Gd_2O_3 nanoparticles with a diameter of 30 to 40 nm, which were compared with Magnovist. The results showed that these nanoparticles have a longer shelf life compared to Magnovist and exhibit the same level of toxicity. Additionally, they create a better contrast in tumors and are excreted through the liver, unlike Magnovist which is excreted through the kidneys. Overall, the study confirmed the potential of these nanoparticles for use in preclinical applications [50].

In 2016, Zhu and colleagues synthesized gadolinium oxide nanoparticles coated with dextran, which had a very fine size of 1.5 nm and a hydrodynamic size of 12.4 nm. In the field of 1.5 Tesla, the r_1 and r_2/r_1 ratio obtained were 12.2 and 2.4 $mM^{-1}s^{-1}$, respectively. The dextran coating made these nanoparticles more biocompatible compared to other gadolinium-based contrast agents. This study suggests that these biocompatible nanoparticles could be used as T_1-weighted contrast agents, highlighting their potential in biomedical imaging applications [51].

4.4 Composition of Gd and Fe_3O_4 nanoparticles

A study conducted by Zhou and colleagues in China in 2015 investigated gadolinium oxide nanoparticles (Gd_2O_3) implanted in iron oxide nanoplates both in vitro on SMCC-7721 cells and in vivo on mice and rats. MRI imaging performed in different fields of 0.5, 3, 7, and 9.4 Tesla, and the r_1 and r_2 values obtained in the field of 3 Tesla and with a dose of 0.2 mg/kg were 20.5 and 145.4 $mM^{-1}s^{-1}$, respectively. The ratio of r_2 to r_1 was 1.7, indicating that GdIOP@ZDS nanoparticles have a high potential to use as T_1 and T_2 contrast agents in MRA [52].

A study conducted by Zhou and colleagues in China in 2012, where they implanted Gd_2O_3 nanoparticles into SPIO nanoparticles, creating GdIO nanoparticles. The study examined the effects of GdIO nanoparticles on HepG2 cells implanted in Nod and BALB/c mice at 7 Tesla. The r_1 and r_2 values for GdIO were 62.5 and 146.5 $mM^{-1}s^{-1}$, respectively, and for Gd_2O_3, 1.12 and 125.4 $mM^{-1}s^{-1}$, respectively. The results demonstrated that these nanoparticles can increase the T_1 and T_2 signal and has a high potential to use as a double contrast material [61].

In 2013, Zhuo and his colleagues conducted a study in China to synthesize gadolinium nanoparticles that were implanted in iron and covered with zwitterin. The study investigated the effects of 4.8 nm diameter nanoparticles on SKOV3 cells of 90 mice. This study promises to revo-

Table 1. Studies have used ultra-small iron oxide as a positive contrast agent.

author	year	r2/r1	Fe_3O_4 size(nm)	group	weighted	field (T)	references
Schnorr J *et al.*	2004	2.4	4	Invivo	T_1 W	1.5	[35]
Kim BH *et al.*	2011	6.12	3	Invivo	T_1 W	3	[36]
Rui YP *et al.*	2016	2.93	4.5	Invivo	T_1 W	1.5	[38]
Park EA *et al.*	2017	3.1	3	Invivo	T_1 W	3	[37]
Shen Z *et al.*	2017	2.6	3.6	Invivo	T_1 W	1.5	[39]
Shen Z *et al.*	2018	6.8	5	Invivo	T_1 W	7	[5]
Zhou Z *et al.*	2015	23.4	7.6	Invivo	T_1 W	7	[52]
Zhou Z *et al.*	2013	5.24	4.8	Invivo	T_1 W	7	[53]
Tao CH *et al.*	2019	2.78	4.34	Invivo	T_1 W	0.5	[54]
Bai CH *et al.*	2018	2.8	5	Invivo	T_1 W	7	[55]
Du CH *et al.*	2020	5.35	3.63	Invivo	T_1 W	3	[56]
Xie M *et al.*	2020	4	2.2	Invivo	T_1 W	7	[57]
Li X *et al.*	2019	2.36	2.8	Invivo	T_1 W	0.5	[16]
Wei R *et al.*	2018	3.56	3.2	Invivo	T_1 W	0.5	[58]
Wei R *et al.*	2018	4.48	3.4	Invivo	T_1 W	1.5	[58]
Wei R *et al.*	2018	20.72	2.8	Invivo	T_1 W	3	[58]
Kim BH *et al.*	2011	6.12	3	Invitro	T_1 W	3	[36]
Du CH *et al.*	2020	5.35	3.63	Invitro	T_1 W	3	[56]
Federenko S *et al.*	2018	6.57	6	Invitro	T_1 W	1.5	[59]
Federenko S *et al.*	2018	1.85	6	Invitro	T_1 W	0.47	[59]
Luo Y *et al.*	2015	4.45	2.7	Invitro	T_1 W	0.5	[60]
Li X *et al.*	2019	2.36	2.8	Invitro	T_1 W	0.5	[16]

lutionize our understanding of the effects of nanoparticles and their potential for medical applications. The study investigated the effects of 4.8 nm diameter nanoparticles on SKOV3 cells of 90 mice. The r_1 and the ratio of r_2 to r_1 obtained in the 7 Tesla field were 7.85 ($mM^{-1}s^{-1}$) and 5.24, respectively. The results indicated that nanoparticles have high potential as T_1-weighted contrast materials and are durable. They have a relatively long duration in the body (50 minutes) and absorbed by the tumor through passive targeting. Furthermore, they have the possibility of rapid purification through the kidneys [53, 62].

In 2015, Yang and colleagues conducted a study in China using iron oxide nanoparticles (Fe_3O_4), $Gd_2O(CO_3)_2$, and SiO_2 as a dual contrast agent. The study found that the nanoparticles were biocompatible and could be used as a T_1 and T_2 contrast enhancer in 3 Tesla MRI scans, with a high potential for accuracy. The study also observed good biocompatibility of the particles in three different cell lines. The values of r_1 and r_2 obtained with SiO_2 thickness of 20 nm were 32.2 and 208 $mM^{-1}s^{-1}$, respectively [63].

In 2010, Choi *et al.* conducted a study in Korea using core-shell nanoparticles consisting of $MnFe_2O_4$ core (15 nm), $Gd_2O(CO_3)_2$ shell (1.5 nm), and a separate layer of SiO_2 (4, 8, 12, and 20 nm). The obtained r_1 and r_2/r_1 were 1.33 and 8.3 ($mM^{-1}s^{-1}$), respectively. The study demonstrated that these newly developed nanoparticles could utilized as T_1 and T_2 contrast enhancers [64].

In 2018, Shen and his colleagues in China investigated the ability of a nanoparticle for T_1-weighted MRI imaging of tumors. They prepared nanoparticles coated with gadolinium and iron oxide using the coprecipitation method. Then, they targeted these nanoparticles with RGD2. The obtained r_1 and r_2/r_1 were 73 and 1.98 $mM^{-1}s^{-1}$, respectively. The study revealed that these nanoparticles have high potential as a contrast material in T_1-weighted imaging. The nanoparticles are small enough to be easily excreted through the kidneys and are non-toxic [5].

Studies have shown a need for a biocompatible contrast agent is highly compatible with a high r_1 ratio and a low r_2/r_1 ratio for positive contrast MRI images. Based on the research its estimated that very fine ion oxide nanoparticles could be a solution to this need.

5. Conclusion

Magnetic nanoparticles can be used as potential contrast materials for MRI as well as new detectors for imaging [65]. Conventional MRI images provide information about the hydrogen in the body, so the intrinsic signals of healthy tissue and tumor are almost identical, and it is difficult to distinguish healthy tissue from tumor. To improve the quality of MRI images, nanoscale contrast materials were created that can change the position of the magnetic field locally and accelerate the relaxation process. Typically, two variables are used to measure the performance of a contrast agent:

1) Longitudinal relaxation or r_1

2) Comfort relaxation or r_2 / r_1 ratio

A value of r_1 indicates the ability of the contrast agent to increase the signal, and the higher it is, the greater the ability of the nanoparticle to increase the signal, while the ratio r_2 / r_1 confirms the potential of a contrast agent to be used as a positive or negative contrast agent. If this ratio is less than 2, the contrast agent weighs T_1 and if it is greater than 10, the contrast agent weighs T_2 [66]. T_2-weight images are dark images that can be confused with bleeding or calcifications. Also, due to the high magnetic momentum of the contrast material used in T_2-weight images, an artifact is seen in the images called the sunrise

effect. T_1-weight contrast agents are generally desirable for reasons such as brighter images, better resolution, and easier detection [39, 67]. But T_1-weight contrast media used in the clinic are usually based on gadolinium ions, which have its drawbacks. Gadolinium-based contrast agents, due to their small size, have a short half-life and are rapidly eliminated from the body, which limits the accurate diagnosis of the tumor as well as long-term monitoring [66–68]. More recent studies have also shown that gadolinium can be found in patients' brains, depending on the dose. Therefore, the FDA issues a general warning for all gadolinium-based substances and prohibits their use in patients with acute renal failure [18, 69]. Gadolinium-based contrast media is available in the clinic and has a low r_1 of about 4, which should be increased to have clearer images [39, 70]. As a result, the need for a high compatibility biocompatibility contrast agent with a high r_1 and a low r_2 / r_1 ratio is fully felt. Many studies have been performed on iron oxide for use as a T_1-weighted contrast agent. The physical properties of iron oxide depend greatly on the size of the iron. When the size of iron oxide is less than 5 nm due to volume reduction, magnetic anisotropy, and spin tilt, the property of iron oxide changes from superparamagnetic to paramagnetic. Due to the high biocompatibility of iron oxide, it has a high potential for use as a T_1-weighted contrast agent. The main problem with these nanoparticles is the low rate of r_1 and the high rate of r_2 / r_1. To solve this problem, they can be combined with gadolinium oxide or gadolinium nanoparticles. Iron oxide nanoparticles are commonly used in medical applications as super-magnetic magnets (Fe_3O_4) and hematite (Fe_2O_3). Studies that have used ultra-small iron oxide as a positive contrast agent are listed in Table 1.

Ethical Approval
This manuscript does not report on or involve the use of any animal or human data or tissue. So the ethical approval is not applicable.

Funding
No funding was received to assist with conducting this study and the preparation of this manuscript.

Authors Contributions
All authors have contributed equally to prepare the paper.

Availability of Data and Materials
The data that support the findings of this study are available from the corresponding author upon reasonable request.

Conflict of Interests
The authors declare that they have no known competing financial interests or personal relationships that could have appeared to influence the work reported in this paper.

Open Access

References

[1] F. Islami, K.D. Miller, R.L. Siegel, Z. Zheng, J. Zhao, X. Han, J. Ma, A. Jemal, and K.R. Yabroff. National and state estimates of lost earnings from cancer deaths in the united states. *JAMA Oncolog*, **5**:e191460, 2019. DOI: https://doi.org/10.1001/jamaoncol.2019.1460.

[2] R.L. Siegel, K.D. Miller, H.E. Fuchs, and A. Jemal. Cancer statistics, CA. *Cancer J. Clin*, 72:7–33, 2022. DOI: https://doi.org/10.3322/caac.21708.

[3] D.L. Hill, D.J. Hawkes, M.J. Gleeson, T.C. Cox, A.J. Strong, W.L. Wong, and A. Sofat. Accurate frameless registration of MR and CT images of the head: Applications in planning surgery and radiation therapy. *Radiol*, **191**:447–454, 1994. DOI: https://doi.org/10.1021/acs.jpclett.0c00143.

[4] X. Gu, D.D. Li, G.H. Yeoh, R.A. Taylor, and V. Timchenko. Heat generation in single magnetic nanoparticles under near-infrared irradiation. *J. Phys. Chem. Lett*, **11**:2182–2187, 2020. DOI: https://doi.org/10.1021/acs.jpclett.0c00143.

[5] Z. Shen, J. Song, Z. Zhou, B.C. Yung, M.A. Aronova, Y. Li, Y. Dai, W. Fan, Y. Liu, Z. Li, H. Ruan, R.D. Leapman, L. Lin, G. Niu, X. Chen, and A. Wu. Dotted core–shell nanoparticles for T_1-weighted MRI of tumors. *Adv. Mater*, **30**:e1803163, 2018. DOI: https://doi.org/10.1002/adma.201803163.

[6] J.S. Ananta, B. Godin, R. Sethi, L. Moriggi, X. Liu, R.E. Serda, R. Krishnamurthy, R. Muthupillai, R.D. Bolskar, L. Helm, M. Ferrari, L.J. Wilson, and P. Decuzzi. Geometrical confinement of gadolinium-based contrast agents in nanoporous particles enhances T_1 contrast. *Nat. Nanotechnol*, **5**:815–821, 2010. DOI: https://doi.org/10.1038/nnano.2010.203.

[7] J.A. Sherwood, M.C. Rich, K. Lovas, J.M. Warram, M.S. Bolding, and Y. Bao. T_1-enhanced MRI-visible nanoclusters for imaging-guided drug delivery. *Nanoscale*, **9**:11785–11792, 2017.

[8] Y. Sun, H.S. Kim, S. Kang, Y.J. Piao, S. Jon, and W.K. Moon. Magnetic resonance imaging-guided drug delivery to breast cancer stem-like cells. *Adv. Healthc. Mater*, **7**:e1800266, 2018. DOI: https://doi.org/10.1002/adhm.201800266.

[9] H. Struyfs, D.M. Sima, M. Wittens, A. Ribbens, N. Pedrosa de Barros, T.V. Phan, M.I. Ferraz Meyer, L. Claes, E. Niemantsverdriet, S. Engelborghs, W. Van Hecke, and D. Smeets. Automated MRI volumetry as a diagnostic tool for Alzheimer's disease: Validation of icobrain dm. *Neuroimage Clin*, **26**:102243–102247, 2020. DOI: https://doi.org/10.1016/j.nicl.2020.102243.

[10] K. Liu, L. Dong, Y. Xu, X. Yan, F. Li, Y. Lu, W. Tao, H. Peng, Y. Wu, Y. Su, D. Ling, T. He, H. Qian, and S. Yu. Stable gadolinium based nanoscale lyophilized injection for enhanced MR angiography with efficient renal clearance. *Biomater*, **158**:74–85, 2018. DOI: https://doi.org/10.1016/j.biomaterials.2017.12.023.

[11] D. Ni, Z. Shen, J. Zhang, C. Zhang, R. Wu, J. Liu, and W. Bu. Integrating anatomic and functional dual-mode magnetic resonance imaging: design and applicability of a bifunctional contrast agent. *ACS Nano*, **10**:3783–3790, 2016. DOI: https://doi.org/10.1021/acsnano.6b00462.

[12] G. Huang, H. Li, J. Chen, Z. Zhao, L. Yang, X. Chi, Z. Chen, X. Wang, and J. Gao. Tunable T_1 and T_2 contrast abilities of manganese-engineered iron oxide nanoparticles through size control. *Nanoscale*, **17**:10404–10412, 2014. DOI: https://doi.org/10.1039/c4nr02680b.

[13] P. Mi, D. Kokuryo, H. Cabral, H. Wu, Y. Terada, T. Saga, and K. Kataoka. A pH-activatable nanoparticle with signal-amplification capabilities for non-invasive imaging of tumour malignancy. *Nat. Nanotechnol*, **11**:724–730, 2016. DOI: https://doi.org/10.1038/nnano.2016.72.

[14] H. Zhou, M. Guo, J. Li, F. Qin, Y. Wang, T. Liu, and Y. Liu. Hypoxia-triggered self-assembly of ultrasmall iron oxide nanoparticles to amplify the imaging signal of a tumor. *J. Am. Chem. Soc*, **143**:1846–1853, 2021. DOI: https://doi.org/10.1021/jacs.0c10245.

[15] Z. Han, X. Wu, S. Roelle, C. Chen, W.P. Schiemann, and Z. Lu. Targeted gadofullerene for sensitive magnetic resonance imaging and risk-stratification of breast cancer. *Nat. Commun*, **8**:692–697, 2017. DOI: https://doi.org/10.1038/s41467-017-00741-y.

[16] X. Li, S. Lu, Z. Xiong, Y. Hu, D. Ma, W. Lou, C. Peng, M. Shen, and X. Shi. Light-addressable nanoclusters of ultrasmall iron oxide nanoparticles for enhanced and dynamic magnetic resonance imaging of arthritis. *Adv. Sci*, **6**:1901800, 2019. DOI: https://doi.org/10.1002/advs.201901800.

[17] D. Cohen, R. Mashiach, L. Houben, A. Galisova, Y. Addadi, D. Kain, and A. Bar-Shir. Glyconanofluorides as immunotracers with a tunable core composition for sensitive hotspot magnetic resonance imaging of inflammatory activity. *ACS Nano*, **15**:7563–7574, 2021. DOI: https://doi.org/10.1021/acsnano.1c01040.

[18] J. Wahsner, E.M. Gale, A. Rodríguez-Rodríguez, and P. Caravan. Chemistry of MRI contrast agents: Current challenges and new frontiers. *Chem. Rev*, **119**:957–1057, 2019. DOI: https://doi.org/10.1021/acs.chemrev.8b00363.

[19] Y. Xiao, R. Paudel, J. Liu, C. Ma, Z. Zhang, and S. Zhou. MRI contrast agents: Classification and application (Review). *Int. J. Mol. Med*, **38**:1319–1326, 2016. DOI: https://doi.org/10.3892/ijmm.2016.2744.

[20] K.M. Hasebroock and N.J. Serkova. Toxicity of MRI and CT contrast agents. *Expert Opin. Drug Metab. Toxicol*, **5**:403–416, 2009. DOI: https://doi.org/10.1517/17425250902873796.

[21] S. Rasaneh, H. Rajabi, and F. Johari Daha. Activity estimation in radioimmunotherapy using magnetic nanoparticles. *Chin. J. Cancer Res*, **27**:203–208, 2015. DOI: https://doi.org/10.3978/j.issn.1000-9604.2015.03.06.

[22] S. Rasaneh, H. Rajabi, M.H. Babaei, and S. Akhlaghpoor. MRI contrast agent for molecular imaging of the HER2/neu receptor using targeted magnetic nanoparticles. *J. Nanopart. Res*, **13**:2285–2293, 2011. DOI: https://doi.org/10.1007/s11051-010-9991-5.

[23] H. Rajabi, S. Rasaneh, and S. Salehi. Synthesis and biological evaluation of 99mTc-Chitosan nanoparticles as a potential radiopharmaceutical for liver imaging. *Synth. React. Inorg. Met*, **46**:1450–1454, 2016. DOI: https://doi.org/10.1080/15533174.2015.1137010.

[24] S. Rasaneh and M. Dadras. The possibility of using magnetic nanoparticles to increase the therapeutic efficiency of herceptin antibody. *Biomed. Eng-Biomed. Tech.*, **60**:485–490, 2015. DOI: https://doi.org/10.1515/bmt-2014-0192.

[25] B. Sadeghi. One-Pot synthesis of Ag/Fe_3O_4 nanocomposite: Preparation and characterization. *Adv. Mater. Process*, **5**:82–92, 2009. URL https://api.semanticscholar.org/CorpusID:55006948.

[26] A. Amraee, Z. Alamzadeh, R. Irajirad, A. Sarikhani, H. Ghaznavi, H. Ghadiri Harvani, S. Rabi Mahdavi, S. Shirvalilou, and S. Khoei. Theranostic RGD@ Fe3O4-Au/Gd NPs for the targeted radiotherapy and MR imaging of breast cancer. *Cancer Nanotechnol*, **14**:1–20, 2023. DOI: https://doi.org/10.1186/s12645-023-00214-6.

[27] A. Szpak, S. Fiejdasz, W. Prendota, T. Straczek, C. Kapusta, J.S. Szmyd, M. Nowakowska, and

S. Zapotoczny. T_1–T_2 dual-modal MRI contrast agents based on superparamagnetic iron oxide nanoparticles with surface attached gadolinium complexes. *J. Nanoparticle Res*, **16**:1–11, 2014. DOI: https://doi.org/10.1007/s11051-014-2678-6.

[28] V.P. Torchilin. Recent advances with liposomes as pharmaceutical carriers. *Nat. Rev. Drug Discov*, **4**: 145–160, 2005. DOI: https://doi.org/10.1038/nrd1632.

[29] V.J. Venditto and F.C. Szoka. Cancer nanomedicines: So many papers and so few drugs! *Adv. Drug Deliv. Rev*, **65**:80–88, 2013. DOI: https://doi.org/10.1016/j.addr.2012.09.038.

[30] Y. Matsumura and H. Maeda. A new concept for macromolecular therapeutics in cancer chemotherapy: Mechanism of tumoritropic accumulation of proteins and the antitumor agent smancs. *Expert Opin. Drug Metab. Toxicol*, **46**:6387–92, 1986. URL https://api.semanticscholar.org/CorpusID:7103917.

[31] A.A. Lozano-Pérez, A.L. Gil, S.A. Pérez, N. Cutillas, H. Meyer, M. Pedreño, and J. Ruiz. Antitumor properties of platinum (iv) prodrug-loaded silk fibroin nanoparticles. *Dalton Trans*, **44**:13513–13521, 2015. DOI: https://doi.org/10.1039/c5dt00378d.

[32] L.D. Leserman, J.N. Weinstein, R. Blumenthal, and W.D. Terry. Receptor-mediated endocytosis of antibody-opsonized liposomes by tumor cells. *Proc. Natl. Acad. Sci. U. S. A.*, **77**:4089–4093, 1980. DOI: https://doi.org/10.1073/pnas.77.7.4089.

[33] N. Kamaly, Z. Xiao, P.M. Valencia, A.F. Radovic-Moreno, and O.C. Farokhzad. Targeted polymeric therapeutic nanoparticles: Design, development and clinical translation. *Chem. Soc. Rev*, **41**:2971–3010, 2012. DOI: https://doi.org/10.1039/c2cs15344k.

[34] A. Koshkaryev, R. Sawant, M. Deshpande, and V. Torchilin. Immunoconjugates and long circulating systems: Origins, current state of the art and future directions. *Adv. Drug Deliv. Rev*, **65**:24–35, 2013. DOI: https://doi.org/10.1016/j.addr.2012.08.009.

[35] J. Schnorr, S. Wagner, C. Abramjuk, I. Wojner, T. Schink, T. J. Kroencke, E. Schellenberger, B. Hamm, H. Pilgrimm, and M. Taupitz. Comparison of the iron oxide-based blood-pool contrast medium VSOP-C184 with gadopentetate dimeglumine for first-pass magnetic resonance angiography of the aorta and renal arteries in pigs. *Invest. Radiol*, **39**:546–553, 2004. DOI: https://doi.org/10.1097/01.rli.0000133944.30119.cc.

[36] B.H. Kim, N. Lee, H. Kim, K. An, Y.I. Park, Y. Choi, K. Shin, Y. Lee, S.G. Kwon, H.B. Na, J. Park, T. Ahn, Y.W. Kim, W.K. Moon, S.H. Choi, and T. Hyeon. Large-scale synthesis of uniform and extremely small-sized iron oxide nanoparticles for high-resolution T_1 magnetic resonance imaging contrast agents. *J. Am. Chem. Soc*, **133**:12624–12631, 2011. DOI: https://doi.org/10.1021/ja203340u.

[37] E.A. Park, W. Lee, Y.H. So, Y.S. Lee, B.S. Jeon, K.S. Choi, E.G. Kim, and W.J. Myeong. Extremely small pseudoparamagnetic Iron Oxide nanoparticle as a novel blood pool T_1 magnetic resonance contrast agent for 3 T whole-heart coronary angiography in canines: Comparison with gadoterate meglumine. *Invest. Radiol*, **52**:128–133, 2017. DOI: https://doi.org/10.1097/RLI.0000000000000321.

[38] Y. Rui, B. Liang, F. Hu, J. Xu, Y. Peng, P. Yin, Y. Duan, C. Zhang, and H. Gu. Ultra-large-scale production of ultrasmall superparamagnetic iron oxide nanoparticles for T1-weighted MRI. *RSC Adv*, **6**:22575–22585, 2016. DOI: https://doi.org/10.1039/C6RA00347H.

[39] Z. Shen, T. Chen, X. Ma, W. Ren, Z. Zhou, G. Zhu, A. Zhang, Y. Liu, J. Song, Z. Li, H. Ruan, W. Fan, L. Lin, J. Munasinghe, X. Chen, and A. Wu. Multifunctional theranostic nanoparticles based on exceedingly small magnetic iron oxide nanoparticles for T_1-weighted magnetic resonance imaging and chemotherapy. *ACS nano*, **11**:10992–11004, 2017. DOI: https://doi.org/10.1021/acsnano.7b04924.

[40] T. Vangijzegem, D. Stanicki, S. Boutry, Q. Paternoster, L. Vander Elst, R.N. Muller, and S. Laurent. VSION as high field MRI T_1 contrast agent: Evidence of their potential as positive contrast agent for magnetic resonance angiography. *Nanotechnol*, **29**:265103, 2018. DOI: https://doi.org/10.1088/1361-6528/aabbd0.

[41] M. Wagner, S. Wagner, J. Schnorr, E. Schellenberger, D. Kivelitz, L. Krug, M. Dewey, M. Laule, B. Hamm, and M. Taupitz. Coronary MR angiography using citrate-coated very small superparamagnetic iron oxide particles as blood-pool contrast agent: Initial experience in humans. *J. Magn. Reson. Imaging*, **34**:816–823, 2011. DOI: https://doi.org/10.1002/jmri.22683.

[42] H. Wei, O.T. Bruns, M.G. Kaul, E.C. Hansen, M. Barch, A. Wiśniowska, O. Chen, Y. Chen, N. Li, S. Okada, J.M. Cordero, M. Heine, C.T. Farrar, D.M. Montana, G. Adam, H. Ittrich, A. Jasanoff, P. Nielsen, and M.G. Bawendi. Exceedingly small iron oxide nanoparticles as positive MRI contrast agents. *Proc. Natl. Acad. Sci. U.S.A.*, **114**:2325–2330, 2017. DOI: https://doi.org/10.1073/pnas.1620145114.

[43] F. Li, Z. Liang, J. Liu, J. Sun, X. Hu, M. Zhao, J. Liu, R. Bai, D. Kim, X. Sun, T. Hyeon, and D. Ling. Dynamically reversible Iron Oxide nanoparticle assemblies for targeted amplification of T_1-weighted magnetic resonance imaging of tumors. *Nano Lett*, **19**:4213–4220, 2019. DOI: https://doi.org/10.1073/pnas.1620145114.

[44] J.L. Campbell, J. Arora, S.F. Cowell, A. Garg, P. Eu, S.K. Bhargava, and V. Bansal. Quasi-cubic magnetite/silica core-shell nanoparticles as enhanced MRI contrast agents for cancer imaging. *PloS one*, **6**:e21857, 2011. DOI: https://doi.org/10.1371/journal.pone.0021857.

[45] J. Reguera, D. Jimenez de Aberasturi, M. Henriksen-Lacey, J. Langer, A. Espinosa, B. Szczupak, C. Wilhelm, and L.M. Liz-Marzán. Janus plasmonic-magnetic gold-iron oxide nanoparticles as contrast agents for multimodal imaging. *Nanoscale*, **27**:9467–9480, 2017. DOI: https://doi.org/10.1039/c7nr01406f.

[46] A. Saraswathy, S.S. Nazeer, M. Jeevan, N. Nimi, S. Arumugam, V.S. Harikrishnan, P.R. Varma, and R.S. Jayasree. Citrate coated iron oxide nanoparticles with enhanced relaxivity for in vivo magnetic resonance imaging of liver fibrosis. *Colloids Surf. B*, **117**:216–224, 2014. DOI: https://doi.org/10.1016/j.colsurfb.2014.02.034.

[47] J. Beik, Z. Alamzadeh, M. Mirrahimi, A. Sarikhani, T.S. Ardakani, M. Asadi, R. Irajirad, M. Mirrahimi, V.P. Mahabadi, N. Eslahi, J.W.M. Bulte, H. Ghaznavi, and A. Shakeri-Zadeh. Multifunctional theranostic Graphene Oxide nanoflakes as MR imaging agents with enhanced photothermal and radiosensitizing properties. *ACS Appl. Bio Mater*, **4**:4280–4291, 2021. DOI: https://doi.org/10.1021/acsabm.1c00104.

[48] S.L. Mekuria, T.A. Debele, and H. Tsai. Encapsulation of Gadolinium Oxide nanoparticle (Gd_2O_3) contrasting agents in PAMAM dendrimer templates for enhanced magnetic resonance imaging in vivo. *ACS Appl. Mater. Interf*, **9**:6782–6795, 2017. DOI: https://doi.org/10.1021/acsami.6b14075.

[49] K.B. Ghaghada, M. Ravoori, D. Sabapathy, J. Bankson, V. Kundra, and A. Annapragada. New dual mode gadolinium nanoparticle contrast agent for magnetic resonance imaging. *PloS One*, **4**:e7628, 2009. DOI: https://doi.org/10.1371/journal.pone.0007628.

[50] Y. Dai, C. Wu, S. Wang, Q. Li, M. Zhang, J. Li, and K. Xu. Comparative study on in vivo behavior of PEGylated gadolinium oxide nanoparticles and Magnevist as MRI contrast agent. *Nanomedicine: NBM*, **14**:547–555, 2018. DOI: https://doi.org/10.1016/j.nano.2017.12.005.

[51] W. Xu, X. Miao, I.T. Oh, K.S. Chae, H. Cha, Y. Chang, and G.H. Lee. Dextran-coated ultrasmall Gd_2O_3 nanoparticles as potential T_1 MRI contrast agent. *Chem. Select*, **1**:6086–6091, 2016. DOI: https://doi.org/10.1002/slct.201600832.

[52] Z. Zhou, C. Wu, H. Liu, X. Zhu, Z. Zhao, L. Wang, Y. Xu, H. Ai, and J. Gao. Surface and interfacial engineering of iron oxide nanoplates for highly efficient magnetic resonance angiography. *ACS Nano*, **9**:3012–3022, 2015. DOI: https://doi.org/10.1021/nn507193f.

[53] Z. Zhou, L. Wang, X. Chi, J. Bao, L. Yang, W. Zhao, Z. Chen, X. Wang, X. Chen, and J. Gao. Engineered Iron-Oxide-based nanoparticles as enhanced T_1 contrast agents for efficient tumor imaging. *ACS Nano*, **7**:3287–3296, 2013. DOI: https://doi.org/10.1021/nn305991e.

[54] C. Tao, Q. Zheng, L. An, M. He, J. Lin, Q. Tian, and S. Yang. T_1-weight magnetic resonance imaging performances of iron oxide nanoparticles modified with a natural protein macromolecule and an artificial macromolecule. *J. Nanomater*, **9**:170–175, 2019. DOI: https://doi.org/10.3390/nano9020170.

[55] C. Bai, Z. Jia, L. Song, W. Zhang, Y. Chen, F. Zang, M. Ma, N. Gu, and Y. Zhang. Time-dependent T_1–T_2 switchable magnetic resonance imaging realized by c(RGDyK) modified ultrasmall Fe_3O_4 nanoprobes. *Adv. Funct. Mater*, **28**:1802281, 2018. DOI: https://doi.org/10.1002/adfm.201802281.

[56] C. Du, J. Wang, X. Liu, H. Li, D. Geng, L. Yu, Y. Chen, and J. Zhang. Construction of pepstatin A-conjugated ultrasmall SPIONs for targeted positive MR imaging of epilepsy-overexpressed P-glycoprotein. *Biomater*, **230**:119581, 2020. DOI: https://doi.org/10.1016/j.biomaterials.2019.119581.

[57] M. Xie, Z. Wang, Q. Lu, S. Nie, C.J. Butch, Y. Wang, and B. Dai. Ultracompact iron oxide nanoparticles with a monolayer coating of succinylated heparin: a new class of renal-clearable and nontoxic T_1 agents for high-field MRI. ACS Appl. Mater. *Interf*, **12**:53994–54004, 2020. DOI: https://doi.org/10.1021/acsami.0c12454.

[58] R. Wei, Z. Cai, B.W. Ren, A. Li, H. Lin, K. Zhang, and J. Gao. Biodegradable and renal-clearable hollow porous iron oxide nanoboxes for in vivo imaging. *Chem. Mater*, **30**:7950–7961, 2018. DOI: https://doi.org/10.1021/acs.chemmater.8b03564.

[59] S. Fedorenko, A. Stepanov, R. Zairov, O. Kaman, R. Amirov, I. Nizameev, K. Kholin, I. Ismaev, A. Voloshina, A. Sapunova, M. Kadirov, and A. Mustafina. One-pot embedding of iron oxides and Gd(III) complexes into silica nanoparticles—Morphology and aggregation effects on MRI dual contrasting ability. *Colloids Surf. A: Physicochem. Eng*, **559**:60–67, 2018. DOI: https://doi.org/10.1016/j.colsurfa.2018.09.044.

[60] Y. Luo, J. Yang, Y. Yan, J. Li, M. Shen, G. Zhang, and X. Shi. RGD-functionalized ultrasmall iron oxide nanoparticles for targeted T_1-weighted MR imaging of gliomas. *Nanoscale*, **7**:14538–14546, 2015. DOI: https://doi.org/10.1039/c5nr04003e.

[61] Z. Zhou, D. Huang, J. Bao, Q. Chen, G. Liu, Z. Chen, X. Chen, and J. Gao. A synergistically enhanced t(1) -t(2) dual-modal contrast agent. *Adv. Mater*, **24**:6223–6228, 2012. DOI: https://doi.org/10.1002/adma.201203169.

[62] U. Palani, B. Iruson, S. Balaraman, S. Krishnamoorthy, and M. Elayaperumal. Synthesis and characterization of iron oxide, rare earth erbium oxide, and erbium oxide blended iron oxide nanocomposites for biomedical activity application. *Int. J. Nano Dimens*, **14**:103–114, 2023. DOI: https://doi.org/10.22034/ijnd.2022.1964912.2170.

[63] M. Yang, L. Gao, K. Liu, C. Luo, Y. Wang, L. Yu, H. Peng, and W. Zhang. Characterization of $Fe_3O_4/SiO_2/Gd_2O(CO_3)_2$ core/shell/shell nanoparticles as T_1 and T_2dual mode MRI contrast agent. *Talanta*, **131**:661–665, 2015. DOI: https://doi.org/10.1016/j.talanta.2014.08.042.

[64] J.S. Choi, J.H. Lee, T.H. Shin, H.T. Song, E.Y. Kim, and J. Cheon. Self-confirming "AND" logic nanoparticles for fault-free MRI. *J. Am. Chem. Soc*, **132**:11015–11017, 2010. DOI: https://doi.org/10.1021/ja104503g.

[65] H. Maeda, T. Sawa, and T. Konno. Mechanism of tumor-targeted delivery of macromolecular drugs, including the EPR effect in solid tumor and clinical overview of the prototype polymeric drug SMANCS. *J. Control Release*, **74**:47–61, 2001. DOI: https://doi.org/10.1016/s0168-3659(01)00309-1.

[66] U.I. Tromsdorf, N.C. Bigall, M.G. Kaul, O.T. Bruns, M.S. Nikolic, B. Mollwitz, and W.J. Parak. Size and surface effects on the MRI relaxivity of manganese ferrite nanoparticle contrast agents. *Nano lett*, **7**:2422–2427, 2007. DOI: https://doi.org/10.1021/nl071099b.

[67] H.B. Na, I.C. Song, and T. Hyeon. Inorganic nanoparticles for MRI contrast agents. *Adv. Mater*, **21**:2133–2148, 2009. DOI: https://doi.org/10.1002/adma.200802366.

[68] P. Caravan. Strategies for increasing the sensitivity of gadolinium based MRI contrast agents. *Chem. Soc. Rev*, **35**:512–523, 2006. DOI: https://doi.org/10.1039/b510982p.

[69] I.A. Dekkers, R. Roos, and A.J. Molen. Gadolinium retention after administration of contrast agents based on linear chelators and the recommendations of the European Medicines Agency. *Eur. Radiol*, **28**:1579–1584, 2018. DOI: https://doi.org/10.1007/s00330-017-5065-8.

[70] C. Liu, D.B. Liu, G.X. Long, J.F. Wang, Q. Mei, G.Y. Hu, and H. Qiu. Specific targeting of angiogenesis in lung cancer with RGD-conjugated ultrasmall superparamagnetic iron oxide particles using a 4.7 T magnetic resonance scanner. *Chin. Med. J*, **126**:2242–2247, 2013. DOI: https://doi.org/10.3760/cma.j.issn.0366-6999.20130628.